Electrochemistry Communications 125 (2021) 106988

Contents lists available at ScienceDirect

Electrochemistry Communications

journal homepage: www.elsevier.com/locate/elecom

Full Communication

Revealing the electrocatalytic behaviour by a novel rotating ring-disc electrode (RRDE) subtraction method: A case-study on oxygen reduction using anthraquinone sulfonate

Dominik Wielend *, Helmut Neugebauer, Niyazi Serdar Sariciftci

Linz Institute for Organic Solar Cells (LIOS), Institute of Physical Chemistry, Johannes Kepler University Linz, Altenberger Strasse 69, 4040 Linz, Austria

ARTICLE INFO

Keywords:
Anthraquinone sulfonate
Electrocatalysis
Oxygen reduction
Rotating ring-disc electrode

ABSTRACT

The state-of-the-art procedure for investigating homogenous and heterogeneous electrocatalysts is cyclic voltammetry (CV). However, this technique usually requires an inactive electrode material. One common problem arising e. g. in studying the oxygen reduction reaction (ORR) is the significant background contribution to the overall ORR current provided by many carbon-based and metal-based electrode materials. Furthermore, rotating ring-disc electrodes (RRDEs) made of common materials like glassy carbon/platinum (GC/Pt) can be affected by overlapping reduction potentials on the disc. Interference from overlapping reactions on the ring might also occur, particularly in connection with oxygen reduction and hydrogen peroxide oxidation in ORR studies.

We present herein a novel subtraction method which allows a semi-quantitative description of homogeneous electrocatalysts and helps to overcome the overlapping problems described above using anthraquinone-2-sulfonate (AQS) as a "case study material" for the ORR.

1. Introduction

For decades it has been known that quinones, and especially anthraquinones, are suitable catalysts for the chemical as well as electrochemical production of hydrogen peroxide (H_2O_2) by the reduction of oxygen (O_2) [1–3]. However, as well as the target 2-electron reaction (O_2 to H_2O_2) the direct 4-electron reduction to water, or reduction of H_2O_2 to water, can occur as competing side-reactions [3]. Many metals, such as platinum, prefer the direct 4-electron reduction to water, whereas others, like gold and most carbon-based materials, show a strong tendency towards hydrogen peroxide production (HPP). The HPP behaviour of carbon electrodes has been known for a long time [4] and the explanation for this outcome is presumed to be that reduced quinone moieties on the electrode surface are oxidized by oxygen which is transformed into H_2O_2 [5–7].

In recent years, immobilized quinones have attracted increased attention for electrochemical H_2O_2 production [3,8,9]. Mechanistic studies of physically adsorbed or covalently attached anthraquinone moieties have been reported, proving the quinone–oxygen reduction and oxidation cycle [10–16]. Dissolved anthraquinones have also been reported as redox mediators in photoelectrochemical cells (PEC) for H_2O_2 production [17,18]. Furthermore, quinones are also widely used in other energy storage applications such as sodium batteries [19] or redox-flow batteries [20–22]. Apart from quinones, a number of other redox-active organic compounds have also been used for electrocatalytic [23] and photocatalytic [24,25] HPP.

In contrast to the above-mentioned studies on immobilized quinones, there have been only a limited number of reports dealing solely with the electrocatalytic ORR properties of homogeneously dissolved quinones [26–29]. As most conventional electrode materials themselves show some electrocatalytic ORR activity, studies examining the homogeneous electrocatalytic effect of quinones for the ORR require special electrode materials which have a kinetically hindered ORR. Examples of such electrode materials are boron-doped diamond (BDD) [26–28] or fully surface-modified electrodes [29]. These studies show that the reduced quinone species themselves reduce O_2 to H_2O_2 by homogeneous electron transfer [17,29].

This challenge of overlapping electrochemical features, related on the one hand directly to the electrode material and on the other hand to the quinone electrocatalyst, was the motivation to develop a method for semi-quantitative examination of solely the electrocatalytic effect of homogenous catalysts, and to distinguish between the two overlapping

* Corresponding author.
E-mail address: dominik.wielend@jku.at (D. Wielend).

https://doi.org/10.1016/j.elecom.2021.106988
Received 12 January 2021; Received in revised form 10 February 2021; Accepted 16 February 2021
Available online 2 March 2021

processes. We used the conventional rotating ring-disc electrode (RRDE) method, taking the well-studied compound anthraquinone-2-sulfonate (AQS) [26,28] as an example.

2. Materials and methods

The chemicals sodium anthraquinone-2-sulfonate monohydrate (AQS) (TCI Chemicals), sodium dihydrogen phosphate dihydrate (Sigma Aldrich), disodium hydrogen phosphate (Sigma Aldrich) and hydrogen peroxide (Merck, 30% solution) were used as received. Cyclic voltammetry (CV) experiments were performed using a 3 mm diameter glassy carbon (GC) disc electrode (PalmSens) as the working electrode (WE), a platinum sheet as the counter electrode (CE) and commercial Ag/AgCl (3 M KCl) (BASi) as the reference electrode, operated by a Jaissle potentiostat-galvanostat PGU10V-100 mA. RRDE experiments were performed with an IPS Jaissle PGU BI-1000 bipotentiostat-galvanostat linked to an IPS PI-ControllerTouch unit and an IPS Rotator 2016 rotating unit. A GC disc ($\varnothing = 5$ mm) in polyether ether ketone with a Pt ring ($\varnothing_m = 7$ mm) was used as the WE, a platinum electrode as the CE and a commercial Ag/AgCl (3 M KCl) (Messtechnik Meinsberg) electrode with a Luggin capillary as the RE. Linear sweep voltammetry (LSV) at a scan rate of 10 mV s^{-1} was used in all RRDE experiments.

UV–vis spectroelectrochemistry was carried out in a spectroelectrochemical cell with a 1 mm path length (BASi) using a Pt mesh as the WE, a Pt wire as the CE and Ag/AgCl as a quasi-RE (determined to be +0.19 V vs. SHE). UV–vis absorption studies were performed on a Varian Cary 3G UV–visible spectrophotometer with a scan rate of 1515 nm s^{-1}.

The disc-type WEs were all polished prior to use for 30 s each with Buehler Micropolish II deagglomerated alumina with particle sizes decreasing from 1.0 to 0.05 μm. In between they were rinsed with 18 MΩ water (MQ water) and isopropanol (VWR Chemicals) to remove excess alumina. Before and during all electrochemical experiments, the cell was purged for 1 h with nitrogen (N_2) or oxygen (O_2) (Linde, 5.0).

According to the literature [3,30], the following formulae are used to determine the faradaic efficiency (FE) of an RRDE process:

$$FE(\%) = \frac{I_R/N}{|I_D|} \cdot 100 \quad (1)$$

$$N_{exp} = \frac{I_R}{|I_D|} \quad (2)$$

The experimental determination of N_{exp} using $K_3[Fe(CN)_6]$ as well as the FE of a bare GC have been reported recently [31].

3. Results and discussion

The electrocatalytic activity of water-soluble AQS (structure in Fig. 1a) towards the ORR is well known [26,28]. It was therefore chosen as a "case study" compound for our studies in a 0.1 M phosphate buffer (PB) at pH = 7. Using a standard glassy carbon (GC) electrode, it can be clearly seen from Fig. 1 that the AQS reduction curve overlaps with the ORR curve of the bare GC (without any AQS added). Besides a broader curve (blue line) for a freshly polished (bare) GC under O_2, the combination of AQS/GC under O_2 is also slightly cathodically shifted compared to AQS/GC under N_2.

It can be seen from Fig. 1a that for AQS/GC under O_2 the reductive peak appears to be composed of two merged peaks. This behaviour is more pronounced at the slower scan rates in Fig. 1b (for scan-rate dependent CV scans under N_2 see Fig. S1) while at faster scan rates only one feature is observed.

Fig. 2 shows the initial UV–vis absorption spectrum of AQS under N_2 (red dotted line, right-hand vertical axis). This figure also shows in situ spectroelectrochemistry of AQS, revealing decreasing absorption at 329 nm while broad bands at 380 and 530 nm evolve upon reduction under N_2. In contrast, the broad feature at 530 nm is not observed under O_2 (see Fig. S2 for full spectra). This behaviour is in good agreement with

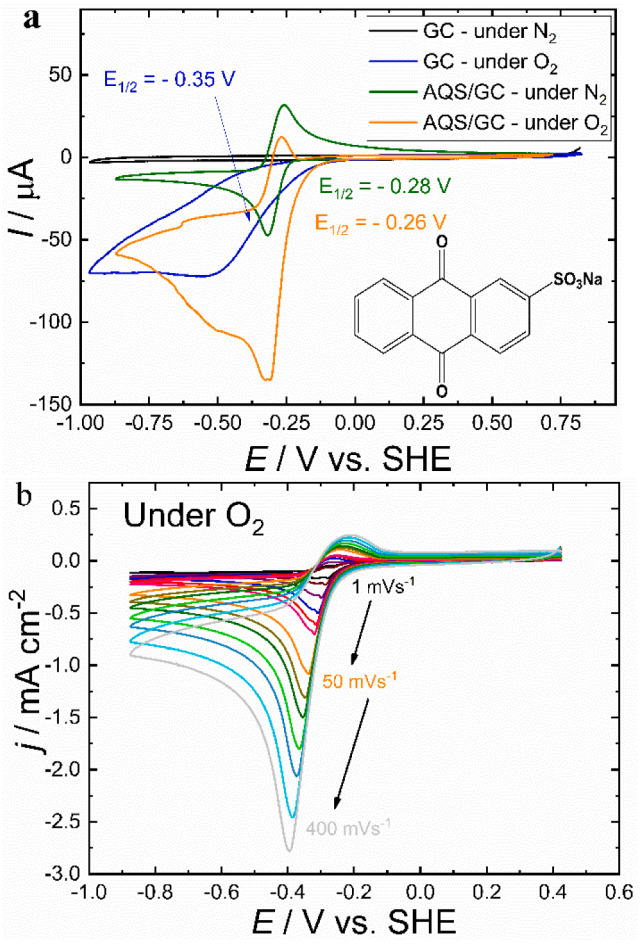

Fig. 1. (a) CV of 1 mM AQS in 0.1 M PB under N_2/O_2 saturated conditions compared with a bare GC under N_2/O_2 saturated conditions recorded at 20 mV s^{-1}. (b) CV scans of 1 mM AQS in 0.1 M PB under O_2 saturated conditions at scan rates between 1 and 400 mV s^{-1}.

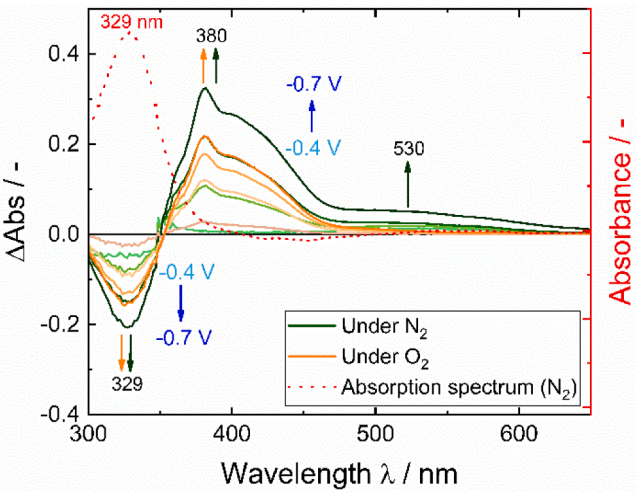

Fig. 2. In situ spectroelectrochemistry of 1 mM AQS under N_2 and under O_2 (differential spectra – left-hand vertical axis), where darker curves correspond to more cathodic potentials. The red dotted line shows the UV–vis absorbance of 1 mM AQS in 0.1 M PB under N_2 (right-hand vertical axis). (For interpretation of the references to colour in this figure legend, the reader is referred to the web version of this article.)

the literature, where the bands at 380 nm correspond to protonated species in this aqueous environment, whereas the active species for the ORR – AQS^{2-} – is expected to absorb at 530 nm [17,32]. These observations indicate that upon addition of O_2 the electrocatalytically active species AQS^{2-} disappears and no stable catalyst–substrate complex is formed.

Due to the overlap of the reduction features when using a GC electrode, CV studies alone cannot provide a clear separation of the electrocatalytic behaviour as the final currents of AQS/O_2 seem to be the sum of AQS/N_2 and GC/O_2. In order to gain more insight into the process, RRDE linear-sweep voltammetry (LSV) was performed. These experiments revealed that the two reduction products on the disc (reduced AQS and H_2O_2) could not be selectively oxidized at the ring by varying the potential. This is because at potentials that are too cathodic (more negative than +0.23 V vs. SHE) the ORR at the Pt ring interferes, while a certain anodic potential (more positive than +0.44 V vs. SHE) would still be required to drive the H_2O_2 oxidation (see Fig. S3). To overcome these limitations and problems, a mathematical method was developed to distinguish between these re-oxidation processes. Moving in this direction, the results in Fig. 3 were obtained at an anodic ring potential at which both reduced species are oxidized (+0.64 V vs. SHE):

The LSV curves in Fig. 3 demonstrate even more clearly that the limiting current of the AQS/O_2 system seems to be additively composed of the AQS/N_2 and GC/O_2 systems. It can be seen that at very cathodic potentials the current of AQS/O_2 (orange curve) is nearly the sum of the current values for AQS/N_2 (green curve) and GC/O_2 (blue curve) in Fig. 3. Qualitatively, the significantly earlier onset of the ORR and the steeper slope (orange curve in Fig. 3) are indications of electrocatalysis by AQS. However, due to the above-mentioned overlap, a quantitative description is not straightforward. For heterogeneous RRDE experiments, the faradaic efficiency for HPP can be calculated via Eq. (1). Here we propose a very similar approach for this model system with homogeneous catalysis (inspired by Fisher [33]) as here the AQS reduction and the ORR overlap.

Since the AQS/O_2 system is linearly composed of the GC/O_2 and AQS/N_2 systems, the difference between this sum and the actual AQS/O_2 data corresponds to an electrocatalytic excess current:

$$I_{\text{excess}} = I_{\text{AQS/O}_2} - \left(I_{\text{GC/O}_2} + I_{\text{AQS/N}_2}\right) \quad (3)$$

According to this excess current in Eq. (3) we are able to calculate the currents for the disc as well as the ring for all rotation speeds. These excess currents are used to calculate the excess efficiency according to Eq. (1), which is illustrated in Fig. 4.

As can be seen from Fig. 4a, as well as from Fig. 3, especially at low overpotentials η, high excess currents are observed which possess a maximum current which then tails off towards zero as soon as the full ORR of the bare GC is established (see Fig. S4 for all plots). According to Fig. 4b, the maximum current peak potentials shift cathodically with increasing ω by roughly 150 mV following a nearly linear trend versus $\omega^{0.5}$, which is usually observed and expected for the current in Levich plots [34]. The origin of the two merged peak behaviour observed for I_D and I_R in some cases is not yet fully understood. As well as the above-mentioned shift in the current maxima, a similar trend is observed in

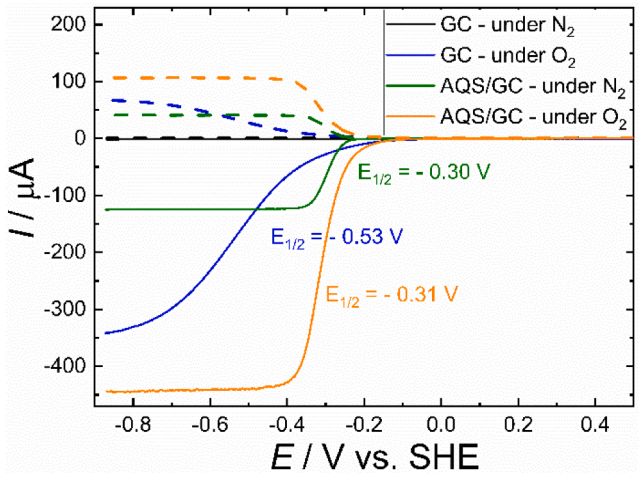

Fig. 3. RRDE-LSV curves of 1 mM AQS in 0.1 M PB at 900 rpm using a scan rate of 10 mV s^{-1} (Ring @ +0.64 V vs. SHE).

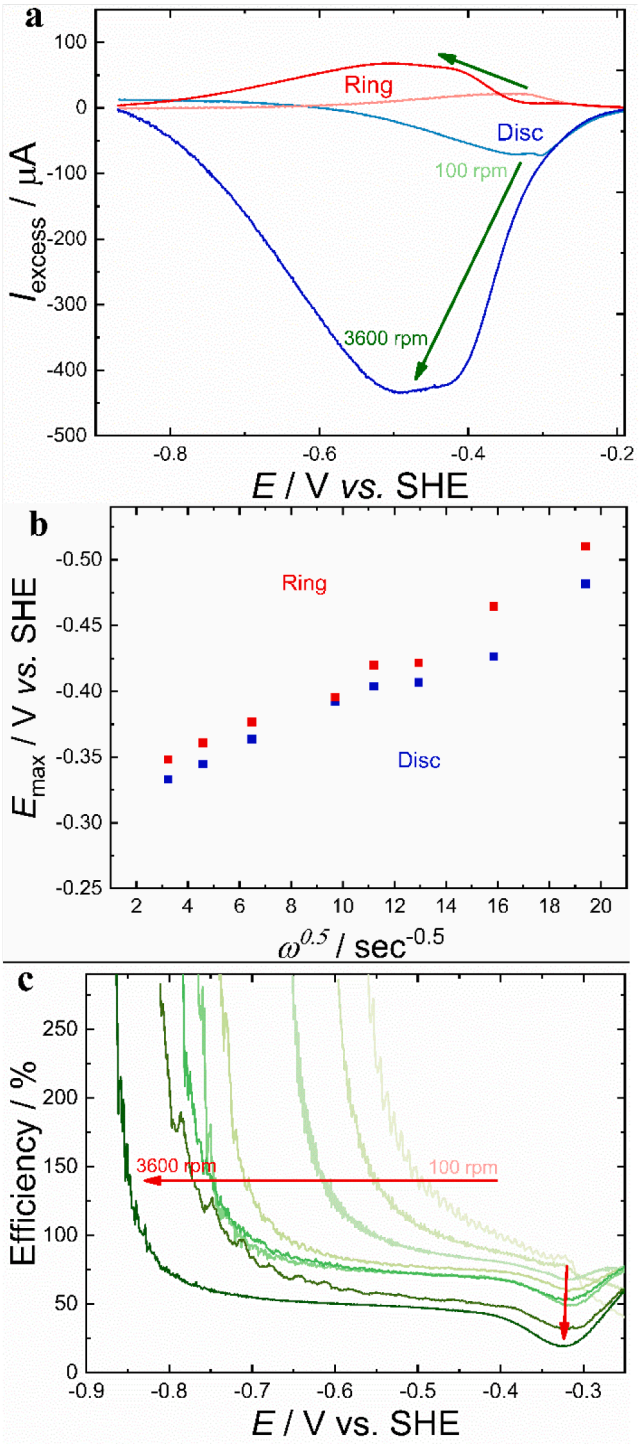

Fig. 4. (a) Calculated excess currents I_D and I_R at 100 and 3600 rpm. (b) Potentials of the maximum current points of I_D and I_R at various rotation speeds versus $\omega^{0.5}$. (c) Calculated excess efficiencies for all rotation speeds between 100 and 3600 rpm.

Fig. 4c for the excess efficiencies. At all rotation speeds, the efficiencies tail off towards high values, which can be even greater than 100%, largely caused by mathematical errors due to the relatively low excess current values at those cathodic potentials. Again, the onset of this tail is cathodically shifted by increasing ω. The shifts and excess current peaks observed on increased convection can be understood by means of the residence time of the AQS molecules in the vicinity of the electrode and the delayed onset of the plain GC ORR, causing flattening of the excess current curves. One unexpected feature in Fig. 4c is the minimum of the excess efficiency at a constant value of 0.32 V, which is not affected by convection. Referring to Fig. 3, this might be the starting potential of AQS reduction without O_2, which is slightly cathodically shifted compared to AQS reduction with O_2 present.

The simple mathematical subtraction method (Eqs. (1) & (3)) described here offers an illustrative insight into the electrocatalytic behaviour of a homogeneous electrocatalyst (here for O_2 to H_2O_2 reduction) in addition to information obtained with classical CV (Fig. 1a) and LSV (Fig. 2). Using these results, a trend of delayed catalytic current and efficiency upon increased convection was demonstrated, in accordance with the well-known Levich equation. The findings illustrated in this work are in agreement with the decreasing residence time of the catalyst in the vicinity of the (disc) electrode at higher rotation speeds.

4. Conclusions

In this work, we investigated the electrocatalytic behaviour of homogenously dissolved anthraquinone sulfonate (AQS) towards "oxygen to hydrogen peroxide" reduction. Usually, when using conventional electrode materials such as glassy carbon (GC) or noble metals, the electrode's ORR (occurring in a non-catalysed way directly at the GC electrode surface) overlaps with the anthraquinone reduction reaction and its electrocatalytic oxygen reduction. To the best of our knowledge, this is the first time that a mathematical subtraction approach has been proposed for the separation of the different current contributions based on RRDE-LSV experimental data and further calculations. Excess currents can be calculated in connection with the electrocatalytic behaviour. It was observed that the maximum excess current potentials are cathodically shifted by increasing the rotation speed. Excess efficiencies close to unity are obtained, cathodically delayed at higher rotation speeds.

Our method provides fast and easy access to parameters that would otherwise be hidden in overlapping contributions and yields results which are in good agreement with literature reports on the use of AQS as a redox mediator for H_2O_2 production under unstirred conditions [17]. Here we have simply demonstrated this method using the well-known electrocatalyst AQS, but we are convinced that this approach could be adopted for routine examination of many other possible homogenous electrocatalytic systems with overlapping redox potentials, without the need to develop specialized electrodes [26,29].

CRediT authorship contribution statement

Dominik Wielend: Conceptualization, Investigation, Writing - original draft. **Helmut Neugebauer:** Validation, Writing - review & editing. **Niyazi Serdar Sariciftci:** Supervision, Funding acquisition, Project administration, Writing - review & editing.

Declaration of Competing Interest

The authors declare that they have no known competing financial interests or personal relationships that could have appeared to influence the work reported in this paper.

Acknowledgements

The authors gratefully acknowledge financial supports from the Austrian Science Foundation (FWF) within the Wittgenstein Prize for Prof. Sariciftci (Z222-N19).

Appendix A. Supplementary data

Supplementary data to this article can be found online at https://doi.org/10.1016/j.elecom.2021.106988.

References

[1] J.M. Campos-Martin, G. Blanco-Brieva, J.L.G. Fierro, Hydrogen peroxide synthesis: an outlook beyond the anthraquinone process, Angew. Chem. Int. Ed. 45 (2006) 6962–6984, https://doi.org/10.1002/anie.200503779.
[2] G. Goor, J. Glenneberg, S. Jacobi, Hydrogen peroxide, Ullmann's Encycl. Ind. Chem. 18 (2012) 393–427, https://doi.org/10.1002/14356007.a13.
[3] A. Sehrish, R. Manzoor, K. Dong, Y. Jiang, Y. Lu, Recent progress on electrochemical production of hydrogen peroxide, Chem. Rep. 1 (2019) 81–101, https://doi.org/10.25082/CR.2019.02.005.
[4] E. Berl, A new cathodic process for the production of H_2O_2, Trans. Electrochem. Soc. 76 (1939) 359, https://doi.org/10.1149/1.3500291.
[5] H. Zhang, C. Lin, L. Sepunaru, C. Batchelor-McAuley, R.G. Compton, Oxygen reduction in alkaline solution at glassy carbon surfaces and the role of adsorbed intermediates, J. Electroanal. Chem. 799 (2017) 53–60, https://doi.org/10.1016/j.jelechem.2017.05.037.
[6] M.S. Hossain, D. Tryk, E. Yeager, The electrochemistry of graphite and modified graphite surfaces: the reduction of O_2, Electrochim. Acta 34 (1989) 1733–1737, https://doi.org/10.1016/0013-4686(89)85057-1.
[7] J. Xu, W. Huang, R.L. McCreery, Isotope and surface preparation effects on alkaline dioxygen reduction at carbon electrodes, J. Electroanal. Chem. 410 (1996) 235–242.
[8] M. Mooste, E. Kibena-Põldsepp, L. Matisen, K. Tammeveski, Oxygen reduction on anthraquinone diazonium compound derivatised multi-walled carbon nanotube and graphene based electrodes, Electroanalysis 29 (2017) 548–558, https://doi.org/10.1002/elan.201600451.
[9] D. Wielend, M. Vera-Hidalgo, H. Seelajaroen, N.S. Sariciftci, E.M. Pérez, D. R. Whang, Mechanically interlocked carbon nanotubes as a stable electrocatalytic platform for oxygen reduction, ACS Appl. Mater. Interfaces 12 (2020) 32615–32621, https://doi.org/10.1021/acsami.0c06516.
[10] K. Tammeveski, K. Kontturi, R.J. Nichols, R.J. Potter, D.J. Schiffrin, Surface redox catalysis for O_2 reduction on quinone-modified glassy carbon electrodes, J. Electroanal. Chem. 515 (2001) 101–112, https://doi.org/10.1016/S0022-0728(01)00633-7.
[11] F. Mirkhalaf, K. Tammeveski, D.J. Schiffrin, Substituent effects on the electrocatalytic reduction of oxygen on quinone-modified glassy carbon electrodes, Phys. Chem. Chem. Phys. 6 (2004) 1321–1327, https://doi.org/10.1039/b315963a.
[12] A. Sarapuu, K. Helstein, K. Vaik, D.J. Schiffrin, K. Tammeveski, Electrocatalysis of oxygen reduction by quinones adsorbed on highly oriented pyrolytic graphite electrodes, Electrochim. Acta 55 (2010) 6376–6382, https://doi.org/10.1016/j.electacta.2010.06.055.
[13] T. Wilson, J. Zhang, C.C. Oloman, D.D.M. Wayner, Anthraquinone-2-carboxylic-allyl ester as a new electrocatalyst for dioxygen reduction to produce H_2O_2, Int. J. Electrochem. Sci. 1 (2006) 99–109.
[14] B. Šljukić, C.E. Banks, R.G. Compton, An overview of the electrochemical reduction of oxygen at carbon-based modified electrodes, J. Iran. Chem. Soc. 2 (2005) 1–25.
[15] Q. Li, C. Batchelor-McAuley, N.S. Lawrence, R.S. Hartshorne, C.J.V. Jones, R. G. Compton, A flow system for hydrogen peroxide production at reticulated vitreous carbon via electroreduction of oxygen, J. Solid State Electrochem. 18 (2014) 1215–1221, https://doi.org/10.1007/s10008-013-2250-9.
[16] P. Manisankar, A. Gomathi, Electrocatalysis of oxygen reduction at polypyrrole modified glassy carbon electrode in anthraquinone solutions, J. Mol. Catal. A 232 (2005) 45–52, https://doi.org/10.1016/j.molcata.2005.01.001.
[17] J. Sun, Y. Wu, Anthraquinone redox relay for dye-sensitized photoelectrochemical H_2O_2 production, Angew. Chem. 132 (2020) 10996–11000, https://doi.org/10.1002/ange.202003745.
[18] P. Chowdhury, P. Fortin, G. Suppes, S. Holdcroft, Aqueous photoelectrochemical reduction of anthraquinone disulfonate at organic polymer films, Macromol. Chem. Phys. 217 (2016) 1119–1127, https://doi.org/10.1002/macp.201500440.
[19] D. Werner, D.H. Apaydin, E. Portenkirchner, An anthraquinone/carbon fiber composite as cathode material for rechargeable sodium-ion batteries, Batteries Supercaps 1 (2018) 160–168, https://doi.org/10.1002/batt.201800057.
[20] S. Schwan, D. Schröder, H.A. Wegner, J. Janek, D. Mollenhauer, Substituent pattern effects on the redox potentials of quinone-based active materials for aqueous redox flow batteries, ChemSusChem (2020) 5480–5488, https://doi.org/10.1002/cssc.202000454.
[21] W.D. McCulloch, M. Yu, Y. Wu, pH-tuning a solar redox flow battery for integrated energy conversion and storage, ACS Energy Lett. 1 (2016) 578–582, https://doi.org/10.1021/acsenergylett.6b00296.

[22] S. Gentil, D. Reynard, H.H. Girault, Aqueous organic and redox-mediated redox flow batteries: a review, Curr. Opin. Electrochem. 21 (2020) 7–13, https://doi.org/10.1016/j.coelec.2019.12.006.
[23] M. Jakešová, D.H. Apaydin, M. Sytnyk, K.T. Oppelt, W. Heiss, N.S. Sariciftci, E. D. Głowacki, Hydrogen-bonded organic semiconductors as stable photoelectrocatalysts for efficient hydrogen peroxide photosynthesis, Adv. Funct. Mater. 26 (2016) 5248–5254, https://doi.org/10.1002/adfm.201601946.
[24] M. Gryszel, M. Sytnyk, M. Jakešová, G. Romanazzi, R. Gabrielsson, W. Heiss, E. D. Głowacki, General observation of photocatalytic oxygen reduction to hydrogen peroxide by organic semiconductor thin films and colloidal crystals, ACS Appl. Mater. Interfaces 10 (2018) 13253–13257, https://doi.org/10.1021/acsami.8b01295.
[25] M. Gryszel, R. Rybakiewicz, E.D. Głowacki, Water-soluble organic dyes as molecular photocatalysts for H_2O_2 evolution, Adv. Sustain. Syst. 3 (2019) 1900027, https://doi.org/10.1002/adsu.201900027.
[26] Q. Li, C. Batchelor-McAuley, N.S. Lawrence, R.S. Hartshorne, R.G. Compton, Semiquinone intermediates in the two-electron reduction of quinones in aqueous media and their exceptionally high reactivity towards oxygen reduction, ChemPhysChem 12 (2011) 1255–1257, https://doi.org/10.1002/cphc.201100174.
[27] C. Batchelor-McAuley, I.B. Dimov, L. Aldous, R.G. Compton, The electrochemistry of quinizarin revealed through its mediated reduction of oxygen, Proc. Natl. Acad. Sci. U.S.A. 108 (2011) 19891–19895, https://doi.org/10.1073/pnas.1113615108.
[28] Q. Li, C. Batchelor-McAuley, N.S. Lawrence, R.S. Hartshorne, R.G. Compton, Electrolyte tuning of electrode potentials: the one electron vs. two electron reduction of anthraquinone-2-sulfonate in aqueous media, Chem. Commun. 47 (2011) 11426–11428, https://doi.org/10.1039/c1cc14191k.
[29] J. Mason, C. Batchelor-McAuley, R.G. Compton, Surface modification imparts selectivity, facilitating redox catalytic studies: quinone mediated oxygen reduction, Phys. Chem. Chem. Phys. 15 (2013) 8362–8366, https://doi.org/10.1039/c3cp50607j.
[30] Y. Sun, I. Sinev, W. Ju, A. Bergmann, S. Dresp, S. Kühl, C. Spöri, H. Schmies, H. Wang, D. Bernsmeier, B. Paul, R. Schmack, R. Kraehnert, B. Roldan Cuenya, P. Strasser, Efficient electrochemical hydrogen peroxide production from molecular oxygen on nitrogen-doped mesoporous carbon catalysts, ACS Catal. 8 (2018) 2844–2856, https://doi.org/10.1021/acscatal.7b03464.
[31] H. Rabl, D. Wielend, S. Tekoglu, H. Seelajaroen, H. Neugebauer, N. Heitzmann, D. H. Apaydin, M.C. Scharber, N.S. Sariciftci, Are polyaniline and polypyrrole electrocatalysts for oxygen (O_2) reduction to hydrogen peroxide (H_2O_2)? ACS Appl. Energy Mater. 3 (2020) 10611–10618, https://doi.org/10.1021/acsaem.0c01663.
[32] R.S.K.A. Gamage, A.J. McQuillan, B.M. Peake, Ultraviolet-visible and electron paramagnetic resonance spectroelectrochemical studies of the reduction products of some anthraquinone sulphonates in aqueous solutions, J. Chem. Soc., Faraday Trans. 87 (1991) 3653–3660, https://doi.org/10.1039/FT9918703653.
[33] A.C. Fisher, Electrode Dynamics, Oxford University Press, Oxford, 1996.
[34] V.G. Levich, Physicochemical Hydrodynamics, Prentice-Hall Inc., Englewood Cliffs, N.J., 1962.